BBA - Biomembranes 1862 (2020) 183200

Contents lists available at ScienceDirect

BBA - Biomembranes

journal homepage: www.elsevier.com/locate/bbamem

Photo-controlled delivery of very long chain fatty acids to cell membranes and modulation of membrane protein function

Li Kong[a], Edgar Dawkins[b], Frederick Campbell[a], Edith Winkler[b], Rico J.E. Derks[d], Martin Giera[d], Frits Kamp[b], Harald Steiner[b,c], Alexander Kros[a,*]

[a] Leiden Institute of Chemistry, Leiden University, 2300 RA Leiden, the Netherlands
[b] Biomedical Center (BMC), Metabolic Biochemistry, Ludwig-Maximilians-University, 81377 Munich, Germany
[c] German Center for Neurodegenerative Diseases (DZNE), 81377 Munich, Germany
[d] Center for Proteomics & Metabolomics, Leiden University Medical Center (LUMC), the Netherlands

ARTICLE INFO

Keywords:
Very long chain fatty acids
Cell membranes
Light activation
γ-Secretase
Alzheimer's disease
Lipidomics
Nervonic acid

ABSTRACT

The biophysical properties and biological functions of membranes are highly dependent on lipid composition. Supplementing cellular membranes with very long chain fatty acids (vlcFAs) is notoriously difficult given the extreme insolubility of vlcFAs in aqueous solution. Herein, we report a solvent-free, photochemical approach to enrich target membranes with vlcFA. To prevent aggregation of vlcFA, we created light-sensitive micelles composed exclusively of poly-ethylene-glycol-nervonic acid amphiphiles (NA-PEG), which spontaneously disassemble in the presence of lipid bilayers. Once embedded within a membrane, UV light is used to cleave off PEG, leaving free nervonic acid (NA, i.e. FA24:1) in the target membrane. When applied to living cells, free NA was processed by the cell to generate various species of membrane and other lipids with incorporated vlcFAs. In this way, we were able to alter the membrane lipid composition of cellular membranes and modulate the enzymatic activity of γ-secretase, an intramembrane protease whose dysfunction has been implicated in the onset and progression of Alzheimer's disease.

1. Introduction

Phospholipid bilayers, as the main constituent of cellular membranes, maintain the structural integrity of cells and are critically important to numerous cellular processes. The activity and function of membrane proteins is dependent on the local properties of the lipid bilayer in which they are embedded [1]. As such, the transmembrane domains (TMD) of many membrane proteins have evolved to prefer a specific lipid bilayer environment [2]. Slight changes of bilayer thickness, fluidity, curvature, and/or lipid headgroup chemistry can therefore lead to destabilization of membrane protein structure and affect function and activity [2–4].

Very long-chain fatty acids (vlcFAs) with a chain-length of ≥22 carbon atoms are important precursors of inflammation-resolving lipid mediators, and play a vital role in cellular functions including spermatogenesis, skin barrier formation and myelin maintenance [5]. Several disorders in the synthesis of vlcFAs (e.g. elongation of stearic acid to saturated or mono-unsaturated vlcFAs) as well as defects in vlcFA metabolism can lead to severe diseases, such as Stargardt disease and adrenoleukodystrophy [5]. Free, unesterified vlcFA can rapidly diffuse across lipid bilayers and redistribute among various cellular compartments [6,7]. When incorporated within endogenous membrane lipids (e.g. sphingo- and glycero-phospholipids), vlcFAs are key modulators of membrane fluidity and thickness, and facilitate the formation of lipid rafts/domains within cell membranes [8]. A change in vlcFA content of a cell membrane may create a hydrophobic mismatch between the lipids and hydrophobic TMDs of embedded membrane proteins [9]. Accordingly, to minimize unfavorable interactions (e.g. exposure of hydrophobic amino acids to water), a change in membrane hydrophobicity may force a membrane protein to alter its state to a more energetically favorable orientation, for instance, by tilting and bending its TMDs in the new membrane landscape. This, in turn, can alter the ability of the protein to carry out its function and, in extreme cases, may lead to a complete loss of function [4]. Thus, the activity of ion channels, transporters and membrane-associated enzymes have all been shown sensitive to changes in lipid membrane composition [10–13].

As acyl-chain remodelling pathways readily incorporate exogenous fatty acids into cellular membrane lipids, delivery of vlcFAs to cells is an attractive option to artificially modulate the physicochemical properties of cell membranes and, thereby, the activity of membrane

* Corresponding author.
E-mail address: a.kros@chem.leidenuniv.nl (A. Kros).

https://doi.org/10.1016/j.bbamem.2020.183200
Received 23 September 2019; Received in revised form 14 January 2020; Accepted 16 January 2020
Available online 20 January 2020

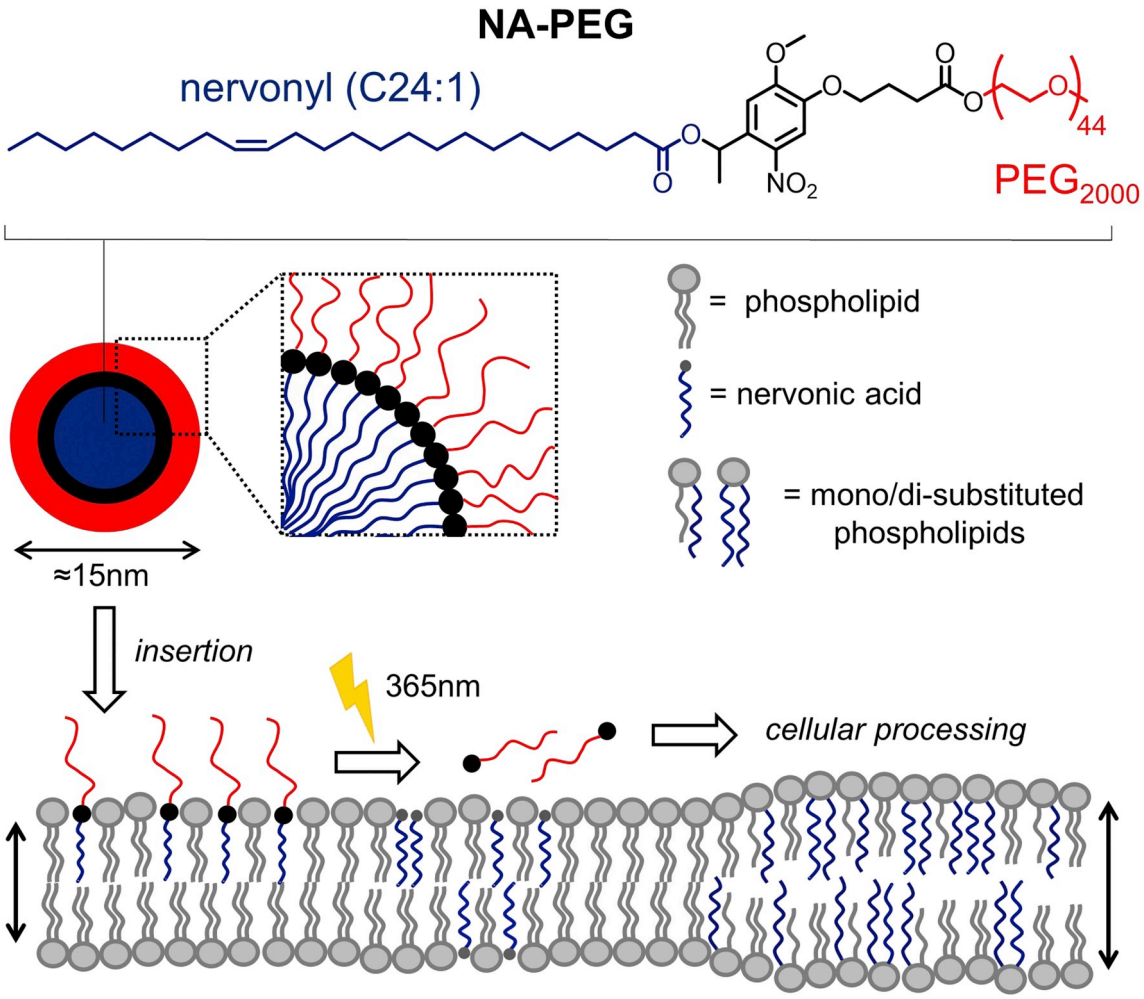

Fig. 1. Delivery, UV-light cleavage of PEG and processing of nervonic acid by target cells. (Top) Chemical structure of light sensitive nervonic acid-PEG conjugate (NA-PEG). (Middle) Self-assembly of NA-PEG to form close packed micelles in aqueous media. (Bottom) Spontaneous disassembly and insertion of NA-PEG micelles in the presence of (cellular) lipid bilayers, followed by light triggered release of free NA and proposed membrane lipid remodelling.

proteins [14,15]. The delivery of vlcFAs to model membranes or cells is, however, complicated by the extreme insolubility of these reagents in aqueous media. This is particularly problematic in the case of vlcFAs with a low degree of unsaturation, e.g. nervonic acid (NA, i.e. FA 24:1). When injected from a solvent (e.g. ethanol or DMSO), these species immediately form insoluble aggregates upon dilution in water. Our motivation for this study was, therefore, to find ways of solubilizing vlcFAs to enable efficient incorporation into target membranes. Once embedded in the plasma membrane, we hypothesized that delivered vlcFAs would be taken up into cellular compartments, enter membrane remodelling pathways [15] and be incorporated into cellular phospholipids. This would, in turn, create larger hydrophobic domains within the lipid bilayer of the cellular membrane and potentially modulate membrane protein activity [3,4].

Herein, we describe a solvent-free method to enrich target membranes with vlcFAs in a photo-inducible manner. To achieve this, NA was chemically conjugated to poly-ethylene-glycol (PEG) via a photo-cleavable (*o*-nitrobenzyl) linker (NA-PEG, Fig. 1) to form vlcFA amphiphiles that self-assemble to close-packed micelles in aqueous media. These micelles spontaneously disassemble in the presence of a lipid bilayer to embed NA-PEG within the target membrane (Fig. 1). Once embedded, photolysis of PEG releases free (i.e. unesterified) NA into the membrane. When we applied our methods to cells, lipidomic analysis demonstrated that free NA was processed by the cell, resulting in elevated levels of vlcFA-containing phospholipids within the cellular membranes. Finally, by altering the lipid composition of cellular membranes in this way, we were able to modulate the enzymatic activity of γ-secretase leading to a reduction of the relative amount of toxic amyloid-β_{42} ($A\beta_{42}$) peptides secreted by treated cells. γ-Secretase dysfunction, and the associated increase in the secretion of $A\beta_{42}$ relative to $A\beta_{40}$ peptides, is widely believed to contribute to the onset and progression of Alzheimer's disease [16,17].

2. Results & discussion

The synthesis and chemical characterization of photolabile, nervonic acid-*o*-nitrobenzyl-PEG_{2000}, NA-PEG, is described in the Experimental procedures (Scheme S1, Fig. S1 – for ^{1}HNMR spectra of NA-PEG, Fig. S2 – for MALDI MS of NA-PEG). Upon UV light irradiation in PBS, complete photolysis was achieved within 30 min (Fig. 2a,b). The appearance of a clear isosbestic point at 320 nm in the UV–Vis absorption spectra indicated clean photoconversion of NA-PEG to its photoproducts. High performance liquid chromatography-evaporative light scattering (HPLC-ELSD) analysis confirmed the expected release of free NA (Fig. 2c). Self-assembly of NA-PEG in aqueous media resulted in close-packed micelles of approximately 15 nm in size (polydispersity index, PDI $<$ 0.2), as determined by dynamic light scattering (DLS, Fig. S4). Micelles, visualized by electron microscopy (Fig. 2d), appeared slightly larger (approx. 25 nm), most likely due to a drying effect during TEM sample preparation. The critical micelle concentration (CMC) of NA-PEG was 2.9 μM (Fig. S3) and particles were stable up to at least 1 mM NA-PEG (Fig. S4).

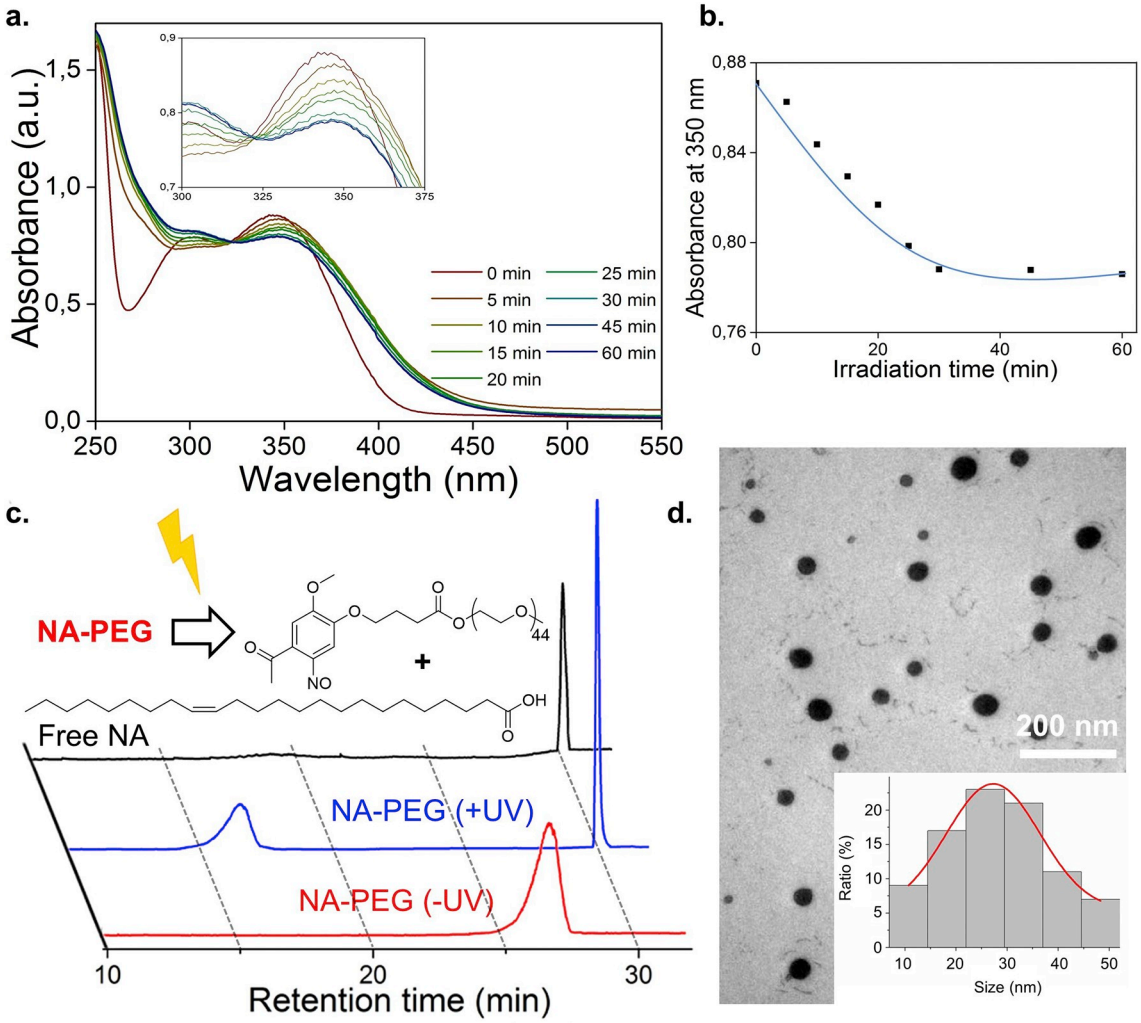

Fig. 2. Photolysis of NA-PEG and biophysical characterization of NA-PEG micelles. (a) Time evolution of the UV–Vis spectra of a solution of NA-PEG during photolysis (365 nm, 3–5 mW/cm^2); (b) Time evolution of the UV absorbance at 350 nm during photolysis. (c) HPLC-ELSD analysis of NA-PEG before (red, single peak) and after UV irradiation (blue; left peak: PEG, right peak NA). HPLC-ELSD analysis of free NA (black, single peak) was used to confirm photolysis of NA-PEG to free NA. (d) TEM images (uranyl acetate stain) of micelles of NA-PEG (500 μM, 1.31 mg ml^{-1}). *Inset*: Size distribution of NA-PEG micelles (n = 90 measured particles), observed by TEM. The average size (diameter) of NA-PEG micelles, as observed by dry TEM is approx. 25 nm.

Next, the incorporation of NA-PEG into model POPC (1-palmitoyl-2-oleoyl-*sn-glycero*-3-phosphocholine) membranes was assessed (Fig. 3a). For this, an aliquot of NA-PEG micelles (1 mM NA-PEG in PBS) was mixed with preformed POPC liposomes (i.e. large unilamellar vesicles, 90 nm, Fig. 3b) at a 1:10 molar ratio (*final concentration*: 100 μM NA-PEG and 1 mM POPC). Successful incorporation of NA-PEG into the POPC liposome membrane was, in part, confirmed by a small increase in the hydrodynamic diameter (D_h) of the liposomes (as measured by DLS), prior to light activation (Fig. 3b). We attribute this to the additional PEG corona presented from the outer leaflet of the POPC liposome membrane. As expected, upon UV light irradiation and photolysis of the PEG corona, the D_h returned to the original size of the parent POPC liposome. Likewise, a significant decrease in measured zeta potential, from −8 mV to −25 mV, was observed following UV radiation of NA-PEG loaded POPC liposomes (Fig. 3c). This can be attributed to the negative charge of the liberated carboxylate headgroup of free NA. Together, these observations confirm successful incorporation of NA into model lipid bilayers by our procedure. In contrast, addition of NA (via ethanol injection) to POPC liposomes resulted in no substantial change to the liposome surface charge (Fig. 3c), highlighting the difficulties of incorporating highly insoluble vlcFAs into lipid membranes by conventional methods [6].

To verify analogous incorporation of NA-PEG into biological membranes, we prepared micelles of NA-PEG containing 1 mol% fluorescently-labeled nervonic acid (NA-Fluo, see Experimental procedures for synthesis and characterization, Fig. S5 for analytical HPLC trace of NA-Fluo). When mixed micelles of NA-PEG and NA-Fluo were incubated with HeLa cells, fluorescence of the cells was immediately observed (Fig. S6). This indicated NA-Fluo spontaneously incorporated into cellular membranes through a process of disassembly of mixed micelles and subsequent transfer of both NA-PEG and NA-Fluo to cellular membranes.

Next, we investigated whether cells could process free NA, following photolysis of NA-PEG delivered to the cell membrane, to generate elevated levels of specific phospholipids with incorporated vlcFAs. Following incubation of NA-PEG (100 μM) and subsequent UV-light cleavage of PEG, cells were incubated to allow for processing and incorporation of the delivered NA into endogenous phospholipids. For this, HEK293 (APPsw) cells, overexpressing Aβ precursor protein (APP), were chosen as these cells were also used in subsequent experiments investigating the impact of changes in membrane lipids on APP processing by γ-secretase (see below). To monitor potential cytotoxicity of NA-PEG + UV treatment, we first looked at acute (3 h after irradiation) vs long term effects (72 h after irradiation) of UV irradiation of cells. Here, we found that 3 h after UV irradiation, cells displayed reduced metabolic activity, as detected by the MTS assay (Fig.

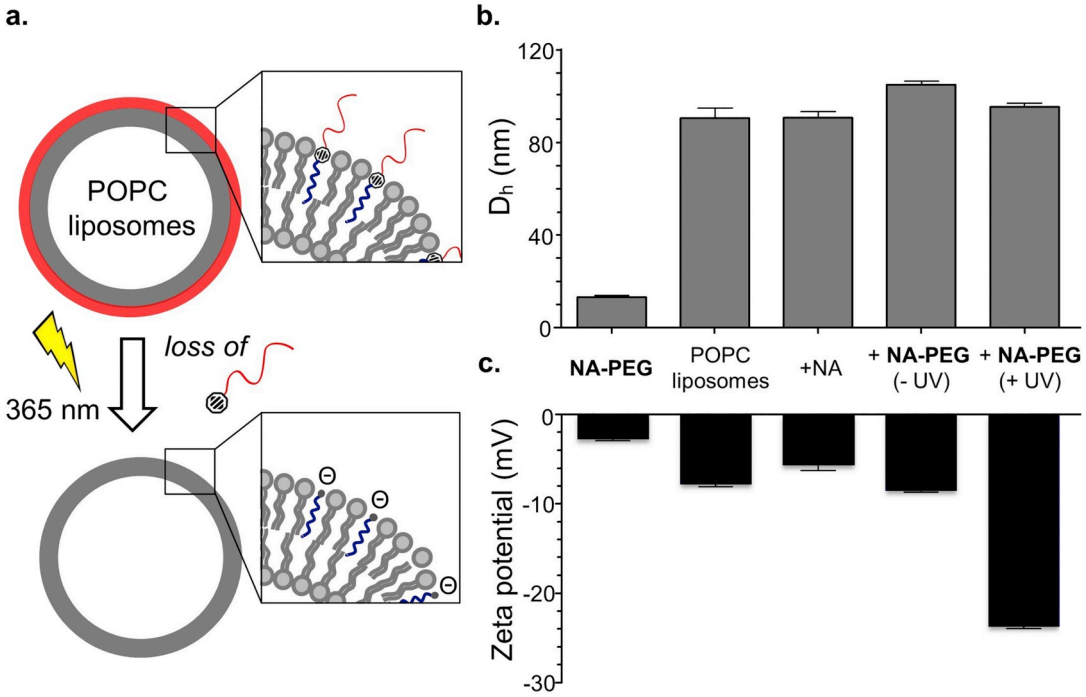

Fig. 3. Incorporation and activation of NA-PEG in model lipid membranes. (a) Cartoon of the procedure. (b) Measured hydrodynamic diameter (D_h) and (c) zeta potentials of micelles of NA-PEG and POPC liposomes. *From l to r*: micelles of NA-PEG, unmodified POPC liposomes, POPC liposomes after ethanol injection of NA, and, alternatively: POPC liposomes incubated with NA-PEG (10:1 molar ratio), followed by UV light irradiation and photolytic loss of PEG.

S7a). Cell viability was dependent on irradiation time (i.e. 10, 20 or 30 min) but also the presence of NA-PEG in the cell membrane. This acute toxicity is most likely caused by a combination of the UV light, NA-PEG in the plasma membrane and/or UV triggered release of large amounts of NA within the cell membrane. However, 72 h after NA-PEG addition, the relative viability of the cells was ~75%, as compared to the PBS control, irrespective of initial 10 min UV irradiation (Fig. S7b). This suggests, after 72 h incubation, cells can recover from the initial stress, continue to grow and thereby process large amount of released NA. Accordingly, following photolysis of NA-PEG delivered to the cell membrane and after 72 h incubation, cells were pelleted and cellular lipids extracted and analyzed by thin layer chromatography (TLC). As shown in Fig. S8, TLC demonstrated that only in the case of treated *and* irradiated cells were substantial amounts of NA incorporated within endogenous PC lipids – the most common class of endogenous phospholipids in cells [18].

To further characterize the specific phospholipid composition of treated cells, we next identified and quantified 265 individual lipid species through LC-MS/MS lipidomic analysis (Fig. 4, for raw data of all lipid species - see Supplementary Table S1). For comparison, we included NA delivered to cells via BSA (i.e. BSA-NA complex), a commonly used method for delivering FA to cells [19]. The lipidomic analysis revealed a large increase of free NA, from very low levels (0.38% in the control) up to 9.1% of the total cellular FA upon treatment with NA-PEG + UV (Fig. 4a, Supplementary Table S1). This was comparable to delivery of NA using BSA (13.6% of cellular FA) (Fig. 4a, Supplementary Table S1). Furthermore, released free NA was processed and incorporated extensively into membrane lipids. Thus, after treatment with NA-PEG + UV, 8.23% of the membrane lipids contained acyl chains with ≥22C-atoms (i.e. contained at least one esterified vlcFA), representing an almost 5.6% increase compared to control (PBS + UV treated) cells (Fig. 4b). This was a larger increase compared to NA delivered via BSA (4.2% increase). For some individual lipid species, the treatment caused a large relative change, for example, the amount of PC 18:1–24:1 was increased 106-fold upon NA-PEG + UV treatment compared to the PBS control, whereas common phospholipid species with long chain FA were reduced (Fig. 4c,d; Supplementary Table S1). Similar effects were achieved for the NA delivery via BSA. The largest shifts in overall acyl chain composition were observed for sphingomyelin (SM) lipids, where the amount of SM d18:1/24:1 increased from 18%, under normal conditions, to 47% of the total observed SM, at the expense of SM d18:1/24:0 and SM d18:1/16:0. Remarkably, changes in these specific SM lipids were much less when NA was delivered via BSA (Fig. 4e). In all cases, changes in the lipidome, as a result of NA-PEG treatment, were mostly acyl chain remodelling events. Thus, in each individual lipid class, minimal changes in the relative proportion of the major membrane lipid classes were observed (Fig. S9). However, a large amount of free NA was incorporated into the triglyceride storage lipids (Fig. S9, Supplementary Table S1). It was also noted that some incorporation of NA was observed in the presence of NA-PEG treated cells which were not UV irradiated. This we attribute to degradation of NA-PEG, which contains a hydrolysable ester bond, within the cell membrane during the 72 h incubation period (Fig. 4a, c–e).

Finally, we investigated whether the enrichment of cellular membranes with vlcFAs could modulate the function of a membrane-associated enzyme. γ-Secretase is a protease which generates Aβ peptides by intramembrane cleavage of the C-terminal fragment (C99) from the amyloid precursor protein (APP) [17]. It is widely believed that the ratio of the production and secretion of toxic $A\beta_{42}$ over less toxic $A\beta_{40}$ and $A\beta_{38}$ species plays an important role in the onset and progression of Alzheimer's Disease (AD) [16,21]. Interestingly, in vitro activity of γ-secretase has been shown to be beneficially modified when the enzyme was reconstituted in thicker model membranes, resulting in a reduced $A\beta_{42}$:$A\beta_{total}$ ratio of released Aβ species [13]. To test whether endogenous γ-secretase activity could be modulated in a similar way (Fig. 5a), HEK293 (APPsw) cells, an APP mutant which has increased production of secreted Aβ [22], were incubated with NA-PEG and subsequently irradiated. After 72 h further incubation, the relative amounts of secreted Aβ peptides were analyzed using a highly specific immunoassay [23]. Here, and only in the case of cells treated with NA-PEG *and* subsequently irradiated, the cleavage precision of C99 processing was significantly altered, resulting in cells producing relatively more $A\beta_{38}$ species, relatively less $A\beta_{42}$ species (Fig. 5b) and a significantly (about 20%) reduced $A\beta_{42}$:$A\beta_{total}$ ratio in the levels of

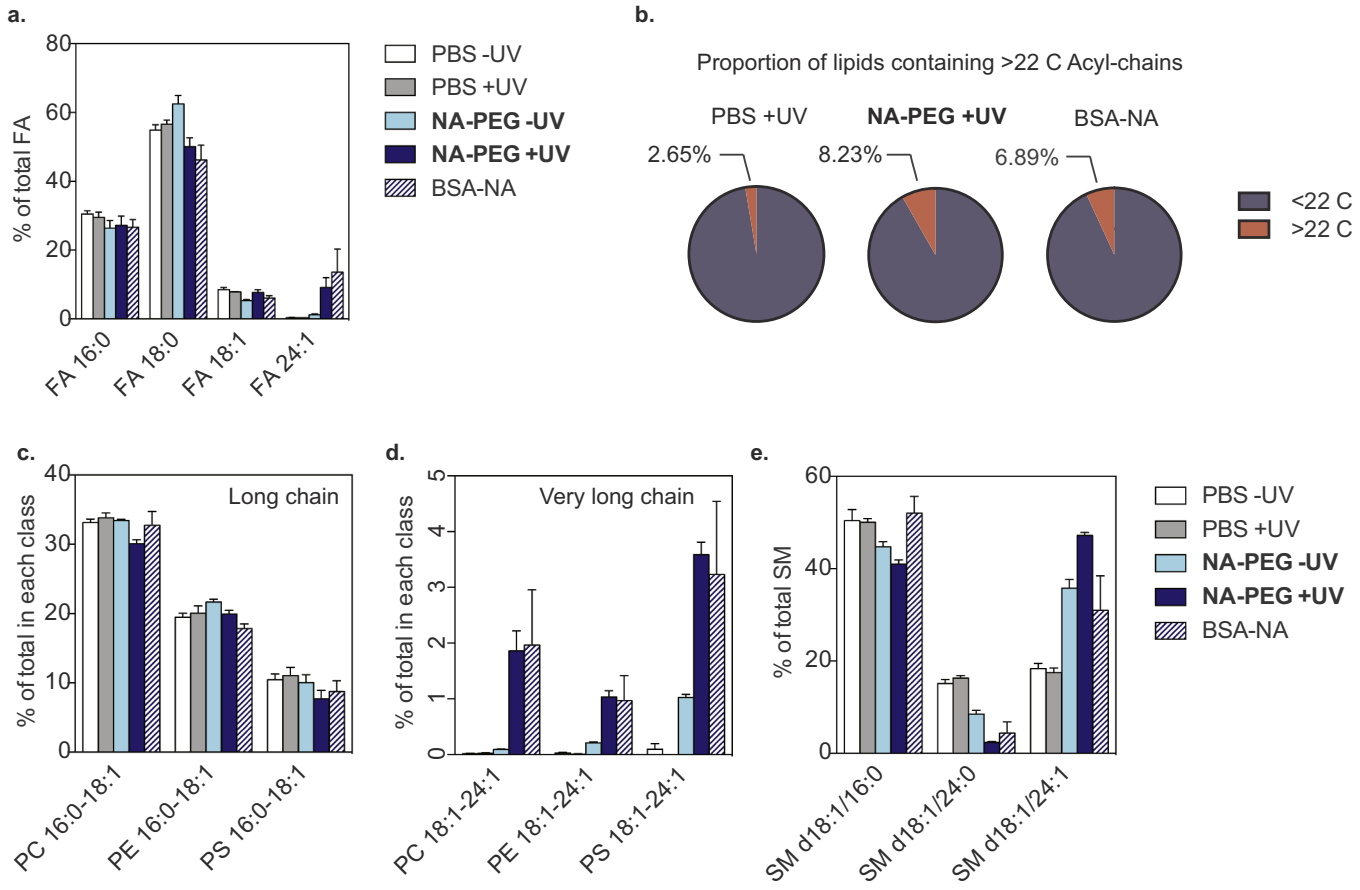

Fig. 4. Membrane remodelling in HEK293 (APPsw) cells following NA-PEG + UV treatment. (a) Relative percentage of different free FA species in the lipid extracts of cells treated with PBS ± UV, NA-PEG ± UV or BSA-NA. (b) Pie chart showing proportion of membrane lipids containing acyl chains < 22C-atoms and ≥22C-atoms, analyzed from the lipid extracts of control (PBS), NA-PEG + UV and BSA-NA treated cells. (c,d) Bar graph showing the percentage of selected, individual (c) long chain (< 22C) and (d) very long chain (≥22C) PC, PE and PS species found in the lipid extracts. (e) Bar graph showing percentage of select SM species. Bars show mean ± SEM, n = 3 independent experiments.

secreted Aβ (Fig. 5c). This change in $A\beta_{42}$:$A\beta_{total}$ ratio mirrored the increased level of incorporated vlcFAs (Fig. 4b). It is, therefore, reasonable to conclude that this 6% increase in membrane lipids containing ≥22C acyl chains may lead to an altered local lipid environment around γ-secretase, leading to approximately 20% reduction in the relative amount of secreted $A\beta_{42}$.

3. Significance

In this work, we demonstrate an efficient, solvent-free method to deliver vlcFAs to target membranes. By applying this method to cells, we show that subsequent cellular processing of delivered vlcFA leads to elevated levels of lipids with incorporated vlcFAs. Increased vlcFA content and membrane remodelling will result in multiple changes to the biophysical properties of the membranes, potentially affecting thickness, surface charge, packing and fluidity. Interestingly, we could demonstrate that the membrane remodelling following NA-PEG treatment resulted in the modification of γ-secretase activity, possibly due to local alterations of the membrane in which γ-secretase is embedded, reducing the relative amount of $A\beta_{42}$, which is thought to be a key factor in AD pathogenesis [16,17].

Our approach has a number of potential advantages for delivering vlcFA to cells over existing methods. Typically, FA species are injected from a concentrated stock solution from ethanol/DMSO, or conjugated to BSA for delivery, which can be toxic to cells [19,24]. Binding of vlcFAs, such as NA to BSA, has been reported to be inefficient, which means that vlcFA require high amounts of BSA for delivery [25]. Furthermore, BSA is able to sequester other lipids from cells, which is avoided by the use of NA-PEG [19]. The lipidomics data presented in this paper show that the effect on membrane remodelling through delivery of free NA via our NA-PEG + UV method is elevated compared to using BSA as a vehicle for NA delivery to cells. In particular, for incorporation of NA in specific targets, such as SM d18:1/24:1, our NA-PEG + UV method was much more effective than BSA-NA. Finally, our new method overcomes the insolubility of extremely hydrophobic molecules and is expected to be transferable to the delivery of any vlcFA or other very hydrophobic lipid species to target membranes. By nature of its UV-activated FA release, we suggest that NA-PEG could also have special applications in live-cell microscopy experiments, for example where the FA can be 'uncaged' in a spatially and temporally-restricted manner using two photon excitation sources. These properties make the PEG delivery of FA reported in this paper an attractive novel approach to studying cellular processes related to disease-related altered levels of vlcFA.

4. Experimental procedures

4.1. Materials and methods

4.1.1. Materials

All chemical reagents, including nervonic acid (NA), were purchased from Sigma Aldrich and used without further purification. Synthetic lipids (POPC (16:0/18:1 PC), diC22:1 (Δ9-cis) PC and diC24:1 (Δ9-cis) PC were purchased from Avanti Polar Lipids. All solvents were

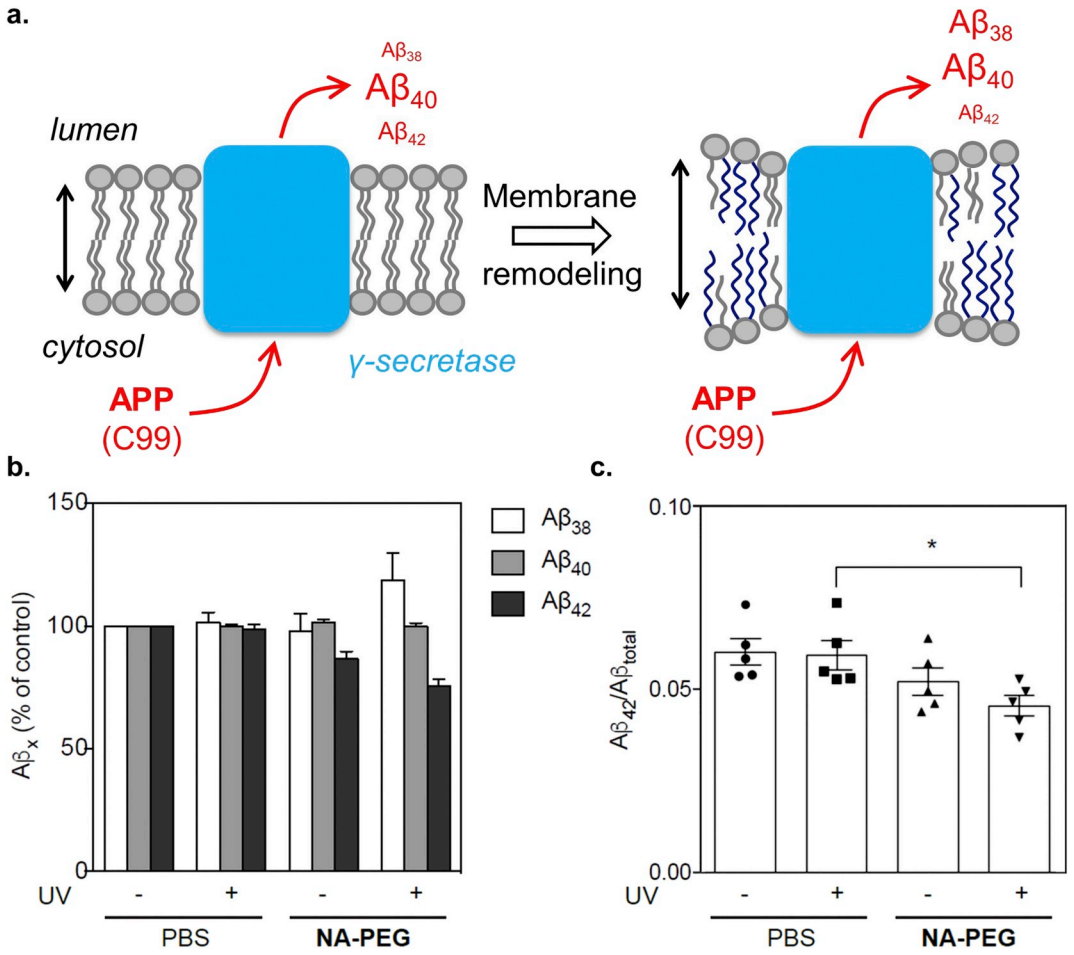

Fig. 5. Modulation of γ-secretase activity through light-triggered alteration of its local lipid environment in HEK293 (APPsw) cell membranes. (a) *Hypothesis*: modulating the local physicochemical properties of HEK293 (APPsw) cell membranes due to elevated incorporation of vlcFA in PC and SM species causes a shift in the relative amounts of different, secreted Aβ species following proteolytic processing of the APP-derived C99 substrate by γ-secretase. (b) Relative changes in $A\beta_{38}$, $A\beta_{40}$ and $A\beta_{42}$ production in the absence/presence of NA-PEG and absence/presence of subsequent UV irradiation. (c) Amount of $A\beta_{42}$ produced relative to total Aβ ($A\beta_{38}$ + $A\beta_{40}$ + $A\beta_{42}$) Bars show mean ± SEM. A significant ($p < 0.05$, students *t*-test, n = 5 independent experiments) reduction in the ratio of $A\beta_{42}/A\beta_{total}$ is only observed for cells treated with NA-PEG *and* subsequently irradiated.

purchased from Biosolve Ltd. Phosphate buffered saline (PBS) contained 5 mM KH_2PO_4, 15 mM K_2HPO_4, 150 mM NaCl, pH 7.4. Silica gel column chromatography was performed using silica gel grade 40–63 μm (Merck). TLC analysis (during synthesis) was performed using aluminum-backed silica gel TLC plates (60_F 254, Merck), visualization by UV absorption at 254 nm and/or staining with $KMnO_4$ solution.

4.1.2. General methods

NMR spectra were measured on a Bruker AV-400 MHz spectrometer. Chemical shifts are recorded in ppm. Tetramethylsilane (TMS) was used as an internal standard. Coupling constants are given in Hz. Analytical High Performance Liquid Chromatography (HPLC) analysis was performed using a Shimadzu HPLC instrument equipped with two LC-8A series pumps coupled to an evaporative light scattering detector (Shimadzu ELSD-LT II detection system). Separation (Vydac 214 MS C4 column, 5 μm, 100 × 4.6 mm, flow rate: 1 ml min^{-1}) using a linear gradient of 10–90% **B** over 20 min followed by a 10 min hold at 90% **B**. Initial 5 min hold at 10% **B**. HPLC buffers: **A**: H_2O (0.1% TFA); **B**: Acetonitrile (0.1% TFA). Flow rate: 1 ml min^{-1}. For characterization of NA-PEG photolysis, the ELSD drift tube temperature was set at 37 °C and the nitrogen flow-rate at 3.5 bar. For NA-Fluo, UV detection at 214 nm was used. UV absorption spectra were measured using a Cary 3 Bio UV–Vis spectrometer, scanning from 250 nm to 550 nm at 1 nm intervals. Scan rate: 150 nm min^{-1}. Particle size distributions and zeta potential measurements were obtained with DLS using a Malvern Zetasizer Nano ZSP. To obtain an estimation of the hydrodynamic diameter ($D_h = 2\ r_h$), the Stokes-Einstein equation was used:

$$D = \frac{k_B T}{6\pi\eta r_h}$$

To obtain the zeta potential (ζ), the Smoluchowski relationship was used:

$$\zeta = \frac{\eta}{\varepsilon}\mu_e$$

where k_B is the Boltzmann constant, η and ε are the viscosity and dielectric constant of the solvent, respectively, and D and μ_e represent the measured diffusion coefficient and electrophoretic mobility of the particle. D_h was calculated from the intensity or number weighed particle size distribution fit of the correlation function, using the Software provided by Malvern Instruments. The polydispersity index (PDI) and Z-averaged D_h was provided by the cumulants fit.

Size measurements were carried out at room temperature at 1 mM total lipid concentration in PBS. For zeta potential measurements, vesicles were diluted 1:10 in 300 mM Sucrose. All reported measurements are the average of three measurements.

MALDI-TOF mass spectra were acquired using an Applied Biosystems Voyager System 6069 MALDI-TOF mass spectrometer. α-Cyano-4-hydroxycinnamic acid was used as matrix in all cases. Sample

concentrations were ~0.3 mg ml^{-1}.

For TEM observation, a drop of NA-PEG (500 μM, PBS) was placed onto a nitrocellulose membrane covered TEM copper grid and dabbed dry through the underside of the grid with a tissue. This was then washed 3 times with ddH_2O. A drop of uranyl acetate (2% w/v) in H_2O was added and the sample left to dry in the dark. Images were obtained at an accelerating voltage of 60 kV (TEM JEOL 1010 instrument).

4.1.3. Light activation of NA-PEG

For experiments not involving cells, UV light irradiation was performed using a hand-held BLAK-RAY B-100AP high intensity UV lamp (365 nm, 100 W, 3–5 $mWcm^{-2}$) encased in a cardboard box. Samples were irradiated in quartz cuvettes at a fixed distance of 10 cm from the UV source. For cell experiments, UV light irradiation was performed using a high-power LED (365 nm, 15–17 $mWcm^{-2}$, Roithner Laser Technik, GmbH) or a 3UV lamp (2.8 $mWcm^{-2}$, 8 W, 230 V, 50 Hz; UVP, Upland, CA, USA) mounted at a fixed distance of 1 cm above the cells.

4.1.4. Micelle, liposome and BSA-NA preparation

Micelles of NA-PEG were prepared via lipid film hydration (PBS) and bath sonication (Branson 2510 Ultrasonic Cleaner, 50 °C, 5 min).

POPC liposomes (10 mM) were prepared via thin film hydration and extrusion at room temperature (Mini-extruder, Avanti Polar Lipids, Alabaster, US). For extrusion, hydrated lipids were passed 11 times through 2 × 400 nm (pore size) polycarbonate membranes (Nucleopore Track-Etch membranes, Whatman), followed by 11 times through 2 × 100 nm polycarbonate to yield large unilamellar vesicles with a diameter of 80–90 nm. POPC liposomes were used immediately after preparation.

BSA-NA complexes were prepared by dropwise addition of a 10 mg ml^{-1} solution of NA in ethanol into a sterile 0.5 mM solution of Fatty Acid Free BSA in PBS, pH 7.4. The solution was incubated at 37 °C for 1 h and stored at −20 °C prior to use.

4.1.5. Cell culture

Cells (HeLa (ATCC® CCL2™); HEK293 (APPsw) [22] were cultivated in Dulbecco's Modified Eagle's Medium (DMEM), supplemented with 2% L-glutamine, 1% penicillin, 1% streptomycin and either 10% fetal calf serum (FCS) and 200 μg ml^{-1} G418 (HEK293 APPsw) or iron supplemented bovine serum (HeLa). Cells were cultured in an atmosphere of 5% CO_2 at 37 °C. Cell culture media were refreshed every two days and cells passaged at 70% confluence by treatment with trypsin-EDTA (0.05% trypsin).

4.2. Synthesis of NA-PEG and NA-Fluo

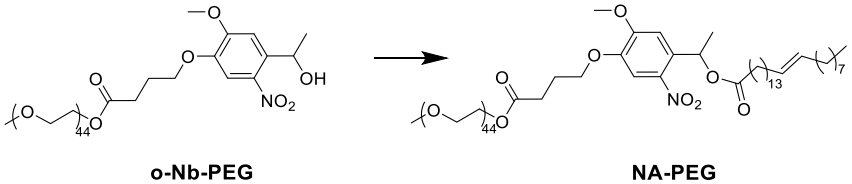

Scheme S1. Methoxy-PEG_{2000}-4-(4-(1-hydroxyethyl)-2-methoxy-5-nitrophenoxy)butanoate (*o*-Nb-PEG) was synthesized as previously reported [26].

4.2.1. Methoxy-PEG_{2000}-4-(2-methoxy-5-nitro-4-(1-(tetracos-15-enoyloxy)ethyl)phenoxy)butanoate (NA-PEG)

To a stirred solution of *o*-Nb-PEG (370 mg, 0.16 mmol) in CH_2Cl_2 (5 ml) was added *4-dimethylaminopyridine* (DMAP, 12.2 mg, 0.1 mmol), 1-ethyl-3-(*3-dimethylaminopropyl*)carbodiimide (EDCI, 57.5 mg, 0.30 mmol), *N,N-diisopropylethylamine* (DIPEA, 78.3 ml, 0.45 mmol) and nervonic acid (92 mg, 0.25 mmol). After overnight stirring, under N_2, the reaction mixture was diluted in EtOAc (50 ml) and washed with sat. $NaHCO_3$ (3 × 50 ml) and brine (50 ml). The organic fractions were combined, dried (Na_2SO_4) and solvent removed under vacuum. Column chromatography (*Gradient*: CH_2Cl_2 to 10% MeOH in CH_2Cl_2) afforded NA-PEG as a light yellow, waxy solid (208 mg, 0.08 mmol, 50%).

R_f: 0.38 (CH_2Cl_2:MeOH; 10:1)

^{1}H NMR ($CDCl_3$, 400 MHz): 7.60 (s, 1H), 7.02 (s, 1H), 6.49 (q, *J = 8 Hz*, 1H), 5.37 (t, *J = 4 Hz*, 1H), 4.28 (m, 2H), 4.13 (t, *J = 4 Hz*, 2H), 4.02 (s, 3H), 3.45–3.95 (m, 174H), 3.41 (s, 3H), 2.60 (t, *J = 4 Hz*, 2H), 2.35 (m, 2H), 2.23 (m, 2H), 2.03 (m, 4H), 1.63 (d, *J = 8 Hz*, 1H), 1.28 (m, 32H), 0.9 (t, *J = 6 Hz*, 3H).

4.2.2. Synthesis of fluorescein-labeled nervonic acid, NA-Fluo

To a stirred solution of nervonic acid (20 mg, 0.05 mmol) in CH_2Cl_2 (2 ml) was added O-(1H-6-chlorobenzotriazole-1-yl)-1,1,3,3-tetramethyluronium hexafluorophosphate (HCTU, 80 mg, 0.2 mmol), DIPEA (70 ml, 0.4 mmol) and fluoresceinamine (70 mg, 0.2 mmol). After stirring for 5 h, the reaction solution was evaporated under vacuum. The residue was redissolved in CH_2Cl_2 (10 ml) and washed with sat. $NaHCO_3$ (3 × 20 ml) and brine (20 ml). Column chromatography (*Gradient*: CH_2Cl_2 to 10% MeOH in CH_2Cl_2), afforded fluorescein-labeled nervonic acid as a yellow solid (15 mg, 0.02 mmol, 45%). Compound purity (judged to be > 90%) was confirmed by analytical HPLC (R_T 29.1 min, Fig. S5).

R_f: 0.27 (CH_2Cl_2:MeOH; 10:1).

ESI-MS $[M + H]^+$: *found*: 696.20, $C_{44}H_{58}NO_6$ *expected*: 696.42.

4.3. Critical micelle concentration (CMC) determination

The CMC was determined by static light scattering (Malvern Zetasizer Nano ZS) through serial dilution of micelles of NA-PEG (from 20 to 7.8 × 10^{-2} μM) in PBS. Measurements were carried out in triplicate at 25 °C. The intensity of scattered light was plotted as a function of the concentration of NA-PEG. The CMC was determined as the intersection of the two plots representing micelles (above the CMC) and free molecules (below the CMC).

4.4. Interaction between micelles of NA-PEG and POPC liposomes

To four separate solutions of preformed POPC liposomes (10 μl, 10 mM in PBS) were added, either a) 90 μl PBS – to give a 1 mM of unmodified POPC liposomes, b) 10 μl of micelles of NA-PEG (1 mM) followed by 80 μl of PBS – to give POPC liposomes modified with NA-PEG (1:10 mol ratio; POPC:NA-PEG) (2 separate samples), or c) 90 μl of PBS followed by 1 μl of nervonic acid (10 mM) in EtOH. The solutions were pipette mixed and left for 15 min at room temperature. b) was subsequently irradiated (365 nm, 3–5 mW cm^{-2}) for 20 min. DLS and zeta potential measurements of all 4 samples were performed immediately.

4.5. Fluorescence imaging of NA delivery of NA-PEG and NA-Fluo to cells

For fluorescence imaging HeLa cells were seeded (1 × 10^5 cells cm^{-2}) in 48-well plates (500 μl, Greiner bio-one, Cellstar®) and

cultured for a further 24 h. Prior to testing, culture medium was carefully removed and the cells washed once with PBS. Micelles of NA-PEG containing 1% of NA-Fluo were prepared by film hydration with PBS and sonication, as for non-fluorescent micelles of NA-PEG. Fluorescently labeled micelles (500 μM total, 5 μM NA-Fluo, 500 μl) were added to HeLa cells and incubated for 20 min. The micelle solution was subsequently removed and cells washed with PBS (3×) and resuspended in DMEM + FCS. Cells were imaged immediately under the fluorescent microscope using an Olympus IX81 fluorescence microscope equipped with a filter cube (Ex. 470/40; Em. 525/50).

4.6. MTS assay

HEK293 (APPsw) cells were plated at a density of 6×10^5 cells cm^{-2} in a 96 well plate and grown for 16 h. Micelles of NA-PEG (100 μM) or PBS vehicle were added for 30 mins, and subsequently the cells were irradiated (varying times, 365 nm, 2.8 mW cm^{-2}). After 1 h or 72 h incubation, MTS cell proliferation reagent (20 μl CellTiter 96® AQueous One Solution Reagent, Promega) was added and the cells were incubated for a further 2 h or 45 mins (72 h incubation). After this incubation time, absorbance was measured at 490 nm according to the supplier guidelines.

4.7. Lipid analysis of cell lysates by TLC

For analysis of cellular lipids, HEK293 (APPsw) cells were seeded (8.6×10^5 cells cm^{-2}) in 12 well plates and cultured for a further 24 h prior to the addition of NA-PEG at a final concentration of 100 μM. After 30 mins, cells were irradiated (10 min, 365 nm, 2.8 mWcm^{-2}) and incubated for a further 72 h. The medium was then changed for 5 h. Cells were then scraped and washed twice in ice-cold PBS by centrifugation at 2500*g* for 10 min at 4 °C. 25–50% of the cell pellet was resuspended in $CHCl_3$:MeOH (1:2). To extract cellular lipids, pellets were briefly (bath) sonicated before centrifugation at 17000*g* for 10 min at 4 °C. The supernatant containing cellular lipids was resolved by TLC using a mobile phase of $CHCl_3$:MeOH:H_2O (65:25:4). In this solvent system, the phospholipids phosphatidylcholine, phosphatidylinositol and phosphatidylserine co-migrate as one spot (PL). Synthetic 24:1 PC, 22:1 PC and POPC were used as standards. TLC analysis was performed using Silica HPTLC plates (Millipore Cat no: 1.05644.001), developed by spraying with 10% $CuSO_4$ (w/v) in 8% phosphoric acid (v/v) and charring at 95 °C overnight on a hot plate. Sarstedt polypropylene reaction tubes (Product no. 72.690.001) were used for lipid extraction.

4.8. Lipidomics

Lipidomic analysis of HEK293 (APPsw) lipid extracts was performed using a LC-MS/MS based lipid profiling method using a Shimadzu Nexera X2 system consisting of LC-30 pumps, a SIL30AC autosampler and a CTO-20AC column oven kept at 50 °C (Shimadzu, 's Hertogenbosch, The Netherlands). A gradient of water/acetonitrile 80:20 v/v (eluent A) and water/acetonitrile/2-propanol 1:90:90 v/v (eluent B) was used. Both eluents contained 5 mM ammonium formate and 0.05% formic acid. The applied gradient, with a column flow of 300 μl min^{-1}, was as follows: 0 min 40% B, 10 min 100% B, 12 min 100% B. A Phenomenex Kinetex C18, 2.7 μm particles, 50 × 2.1 mm (Phenomenex, Utrecht, The Netherlands) was used as column. Lipid extracts were dissolved in 100 μl 2-propanol followed by 5 min of ultrasonification. Subsequently, samples were diluted with 100 μl water and 10 μl was injected into the LC-MS system. The MS was a Sciex TripleTOF 6600 (AB Sciex Netherlands B.V., Nieuwerkerk aan den Ijssel, The Netherlands) operated in positive (ESI+) and negative (ESI−) ESI mode, with the following conditions: Ion Source Gas 1, 2 and Curtain gas 30 psi, temperature 350 °C, acquisition range *m/z* 100–1200, IonSpray Voltage 5500 V (ESI+) and −4500 V (ESI-), declustering potential 80 V (ESI+) and −80 V (ESI−). An information dependent acquisition (IDA) method was used to identify lipids, with the following conditions for MS analysis: collision energy ± 10, acquisition time 250 ms and for MS/MS analysis: collision energy ± 45, collision energy spread 25, ion release delay 30, ion release width 14, acquisition time 40 ms. The IDA switching criteria where set as: for ions greater than *m/z* 300, which exceed 200 cps, exclude former target for 2 s, exclude isotopes within 1.5 Da, max. candidate ions 20.

Before data analysis, raw MS data files where converted with the Reifycs Abf Converter (v1.1) to the Abf file. MS-DIAL (v2.74), with the FiehnO (VS27) database, was used to align the data and identify the different lipids [27]. PC and PE lipids were manually curated to confirm their identity. Due to overlap of triglyceride (TG) species, MS-DIAL could not sufficiently identify lipid species, in turn a modified identification approach was applied. Initially, MS-DIAL was used to get the total number of carbons and double bonds of a TG. This information together with the MS/MS spectrum was used to search the glycerolipid MS/MS predicted database on LipidMaps [28]. TG's with all their neutral loss of lipid species fragments matched where assigned as correctly identified. Raw lipidomics data is included as a separate excel file.

4.9. Analysis of Aβ generation

HEK293 cells overexpressing APPsw were cultured and treated with NA-PEG as outlined above (Section 4.7). Conditioned medium (5 h) was centrifuged at 2500 ×*g* for 10 min to clear cellular debris, prior to analysis by triplex sandwich immunoassay specific for Aβ38, Aβ40, and Aβ42 species (Meso Scale Discovery).

Supplementary data to this article can be found online at https://doi.org/10.1016/j.bbamem.2020.183200.

Declaration of competing interest

The authors declare that they have no known competing financial interests or personal relationships that could have appeared to influence the work reported in this paper.

Acknowledgements

This research was funded by a China Scholarship Council grant (L.K.), the Netherlands Organisation for Scientific Research (NWO-Vici - project nr. 724.014.001, A.K. and F.C.), the Deutsche Forschungsgemeinschaft (STE 847/6-1 grant, H.S.), the Alzheimer Forschung Initiative e.V. (H.S.) and the VERUM Foundation (F.K.).

Author contributions

AK and HS supervised this study. FC, FK, ED, MG, HS and AK designed the experiments and wrote the manuscript with contributions from all authors. LK, ED, EW, RD performed the experiments while all authors were involved in the interpretation of the data.

References

[1] Z. Cournia, T.W. Allen, I. Andricioaei, B. Antonny, D. Baum, G. Brannigan, N.V. Buchete, J.T. Deckman, L. Delemotte, C. del Val, R. Friedman, P. Gkeka, H.C. Hege, J. Hénin, M.A. Kasimova, A. Kolocouris, M.L. Klein, S. Khalid, M.J. Lemieux, N. Lindow, M. Roy, J. Selent, M. Tarek, F. Tofoleanu, S. Vanni, S. Urban, D.J. Wales, J.C. Smith, A.N. Bondar, Membrane protein structure, function, and dynamics: a perspective from experiments and theory, J. Membr. Biol. 248 (2015) 611–640, https://doi.org/10.1007/s00232-015-9802-0.

[2] H.J. Sharpe, T.J. Stevens, S. Munro, A comprehensive comparison of transmembrane domains reveals organelle-specific properties, Cell. 142 (2010) 158–169, https://doi.org/10.1016/j.cell.2010.05.037.

[3] O.S. Andersen, R.E. Koeppe, Bilayer thickness and membrane protein function: an energetic perspective, Annu. Rev. Biophys. Biomol. Struct. 36 (2007) 107–130, https://doi.org/10.1146/annurev.biophys.36.040306.132643.

[4] A.G. Lee, How lipids affect the activities of integral membrane proteins, Biochim. Biophys. Acta Biomembr. 1666 (2004) 62–87, https://doi.org/10.1016/j.bbamem.

2004.05.012.
[5] A. Kihara, Very long-chain fatty acids: elongation, physiology and related disorders, J. Biochem. 152 (2012) 387–395, https://doi.org/10.1093/jb/mvs105.
[6] F. Zhang, F. Kamp, J.A. Hamilton, Dissociation of long and very long chain fatty acids from phospholipid bilayers, Biochemistry. 35 (1996) 16055–16060, https://doi.org/10.1021/bi961685b.
[7] F. Kamp, J.A. Hamilton, How fatty acids of different chain length enter and leave cells by free diffusion, Prostaglandins Leukot. Essent. Fat. Acids 75 (2006) 149–159, https://doi.org/10.1016/j.plefa.2006.05.003.
[8] J.B. de la Serna, G.J. Schütz, C. Eggeling, M. Cebecauer, There is no simple model of the plasma membrane organization, Front, Cell Dev. Biol. 4 (2016) 106, https://doi.org/10.3389/fcell.2016.00106.
[9] J.A. Killian, Hydrophobic mismatch between proteins and lipids in membranes, Biochim. Biophys. Acta Rev. Biomembr. 1376 (1998) 401–415, https://doi.org/10.1016/S0304-4157(98)00017-3.
[10] A. Lee, Lipid–protein interactions in biological membranes: a structural perspective, Biochim. Biophys. Acta Biomembr. 1612 (2003) 1–40, https://doi.org/10.1016/S0005-2736(03)00056-7.
[11] A.G. Lee, Biological membranes: the importance of molecular detail, Trends Biochem. Sci. 36 (2011) 493–500, https://doi.org/10.1016/j.tibs.2011.06.007.
[12] F.X. Contreras, A.M. Ernst, F. Wieland, B. Brügger, Specificity of intramembrane protein-lipid interactions, Cold Spring Harb. Perspect. Biol. 3 (2011) 1–18, https://doi.org/10.1101/cshperspect.a004705.
[13] E. Winkler, F. Kamp, J. Scheuring, A. Ebke, A. Fukumori, H. Steiner, Generation of Alzheimer disease-associated amyloid Aβ 42/43 peptide by γ-secretase can be inhibited directly by modulation of membrane thickness, J. Biol. Chem. 287 (2012) 21326–21334, https://doi.org/10.1074/jbc.M112.356659.
[14] A.A. Spector, R.E. Kiser, G.M. Denning, S.W. Koh, L.E. DeBault, Modification of the fatty acid composition of cultured human fibroblasts, J. Lipid Res. 20 (1979) 536–547 http://www.ncbi.nlm.nih.gov/pubmed/458270.
[15] A. Yamashita, Y. Hayashi, Y. Nemoto-Sasaki, M. Ito, S. Oka, T. Tanikawa, K. Waku, T. Sugiura, Acyltransferases and transacylases that determine the fatty acid composition of glycerolipids and the metabolism of bioactive lipid mediators in mammalian cells and model organisms, Prog. Lipid Res. 53 (2014) 18–81, https://doi.org/10.1016/j.plipres.2013.10.001.
[16] D.J. Selkoe, J. Hardy, The amyloid hypothesis of Alzheimer's disease at 25 years, EMBO Mol. Med. 8 (2016) 595–608, https://doi.org/10.15252/emmm.201606210.
[17] H. Steiner, A. Fukumori, S. Tagami, M. Okochi, Making the final cut: pathogenic amyloid-β peptide generation by γ-secretase, Cell Stress. 2 (2018) 292–310. doi:10.15698/cst2018.11.162.
[18] G. van Meer, D.R. Voelker, G.W. Feigenson, Membrane lipids: where they are and how they behave, Nat. Rev. Mol. Cell Biol. 9 (2008) 112–124, https://doi.org/10.1038/nrm2330.
[19] N. Alsabeeh, B. Chausse, P.A. Kakimoto, A.J. Kowaltowski, O. Shirihai, Cell culture models of fatty acid overload: problems and solutions, Biochim. Biophys. Acta - Mol. Cell Biol, Lipids. (2018) 143–151, https://doi.org/10.1016/j.bbalip.2017.11.006.
[21] N. Tang, K.P. Kepp, Aβ42/Aβ40 ratios of presenilin 1 mutations correlate with clinical onset of Alzheimer's disease, J. Alzheimers Dis. 66 (2018) 939–945, https://doi.org/10.3233/JAD-180829.
[22] M. Citron, T. Oltersdorf, C. Haass, L. McConlogue, A.Y. Hung, P. Seubert, C. Vigo-Pelfrey, I. Lieberburg, D.J. Selkoe, Mutation of the β-amyloid precursor protein in familial Alzheimer's disease increases β-protein production, Nature. 360 (1992) 672–674, https://doi.org/10.1038/360672a0.
[23] R.M. Page, K. Baumann, M. Tomioka, B.I. Pérez-Revuelta, A. Fukumori, H. Jacobsen, A. Flohr, T. Luebbers, L. Ozmen, H. Steiner, C. Haass, Generation of Aβ38 and Aβ42 is independently and differentially affected by familial Alzheimer disease-associated presenilin mutations and γ-secretase modulation, J. Biol. Chem. 283 (2008) 677–683, https://doi.org/10.1074/jbc.M708754200.
[24] C.A. Drevon, D.B. Weinstein, D. Steinberg, Regulation of cholesterol esterification and biosynthesis in monolayer cultures of normal adult rat hepatocytes, J. Biol. Chem. 255 (1980) 9128–9137 www.jbc.org/content/255/19/9128.long.
[25] J.K. Choi, J. Ho, S. Curry, D. Qin, R. Bittman, J.A. Hamilton, Interactions of very long-chain saturated fatty acids with serum albumin, J. Lipid Res. 43 (2002) 1000–1010, https://doi.org/10.1194/jlr.M200041-JLR200.
[26] L. Kong, S.H.C. Askes, S. Bonnet, A. Kros, F. Campbell, Temporal control of membrane fusion through photolabile PEGylation of liposome membranes, Angew. Chem. Int. Ed. 55 (2016) 1396–1400, https://doi.org/10.1002/anie.201509673.
[27] H. Tsugawa, T. Cajka, T. Kind, Y. Ma, B. Higgins, K. Ikeda, M. Kanazawa, J. Vandergheynst, O. Fiehn, M. Arita, MS-DIAL: data-independent MS/MS deconvolution for comprehensive metabolome analysis, Nat. Methods 12 (2015) 523–526, https://doi.org/10.1038/nmeth.3393.
[28] E. Fahy, M. Sud, D. Cotter, S. Subramaniam, LIPID MAPS online tools for lipid research, Nucleic Acids Res. 35 (2007) W606–W612, https://doi.org/10.1093/nar/gkm324.